NANO LETTERS

2008
Vol. 8, No. 3
836-841

Optical Properties of Rotationally Twinned InP Nanowire Heterostructures

Jiming Bao,[†] David C. Bell,[†,‡] and Federico Capasso*[,†]

School of Engineering and Applied Sciences, Center for Nanoscale Systems, Harvard University, Cambridge, Massachusetts 02138

Jakob B. Wagner

nCHREM Polymer and Materials Chemistry, Lund University, PO Box 124, SE-22100 Lund, Sweden

Thomas Mårtensson, Johanna Trägårdh, and Lars Samuelson

Solid State Physics, Lund University, PO Box 118, SE-22100 Lund, Sweden

Received November 8, 2007; Revised Manuscript Received January 18, 2008

ABSTRACT

We have developed a technique so that both transmission electron microscopy and microphotoluminescence can be performed on the same semiconductor nanowire over a large range of optical power, thus allowing us to directly correlate structural and optical properties of rotationally twinned zinc blende InP nanowires. We have constructed the energy band diagram of the resulting multiquantum well heterostructure and have performed detailed quantum mechanical calculations of the electron and hole wave functions. The excitation power dependent blue-shift of the photoluminescence can be explained in terms of the predicted staggered band alignment of the rotationally twinned zinc blende/wurzite InP heterostructure and of the concomitant diagonal transitions between localized electron and hole states responsible for radiative recombination. The ability of rotational twinning to introduce a heterostructure in a chemically homogeneous nanowire material and alter in a major way its optical properties opens new possibilities for band-structure engineering.

Nanotechnology based on semiconductor nanowires has opened up new directions in band gap engineering of optoelectronic devices due to the large design space made possible by the relaxation of many constraints typical of thin film growth.[1–3] However the study of the structural and optical properties of the *same* nanowire, which is essential to correlate them in an unambiguous way, has not yet been performed. In order to establish this correlation, we have developed a special grid so that both high-resolution transmission electron microscopy (HRTEM) and microphotoluminescence (PL) measurements over a large range of optical power can be performed on the *same* nanowire. In contrast to bulk materials, nanowires are electron-transparent without further processing. This is important since sample preparation methods such as mechanical polishing and ion milling may destroy or alter the optical properties. Using the new technique here reported, we have established a direct correlation between the structural and optical properties of rotationally twinned (RT) zinc blende (ZB) InP nanowires.[4–6] RT heterostructures observed in these nanowires are based on a heterojunction consisting of adjacent rotated lattices in InP. The observed power dependent blue shift of the PL spectra can be qualitatively explained by modeling the electron and hole wave functions of the InP nanowire heterostructure based on TEM lattice image and the predicted staggered heterojunction band alignment between ZB InP and twinning associated wurtzite (WZ) InP.[7] RT, if suitably controlled, could add a new dimension in nanostructure device design.[8,9]

Both WZ (*hexagonal*) and ZB (*cubic*) lattices belong to the close-packed crystal structure, and many materials can crystallize in either form or in a mixed structure (so-called polytype) under specific conditions.[10–12] A stacking fault is a type of plane defect in ZB or WZ crystals.[10,13,14] In RT ZB crystals, lattices adjacent to the twin plane have the same ZB structure, but they are rotated 180° around the ⟨111⟩ growth direction.[10,13–15] As shown in Figure 1a, a RT structure can be regarded as one layer of stacking fault.[10,13–15] Stacking faults have been found to contribute to many phenomena, for example, an unexpectedly large photovoltaic effect.[16,17] In the models developed, many of these observations were

* To whom correspondence may be addressed.
† School of Engineering and Applied Sciences.
‡ Center for Nanoscale Systems.

10.1021/nl072921e CCC: $40.75
Published on Web 02/15/2008

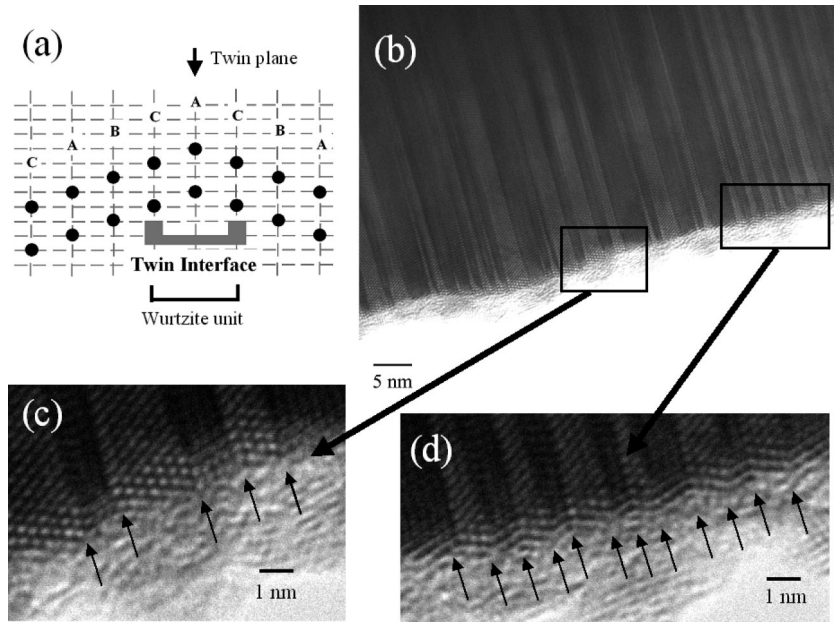

Figure 1. (a) Schematic of the stacking sequence of closely packed planes A, B, and C along the ⟨111⟩ direction near a twin plane in a rotationally twinned zinc blende (ZB) crystal. The CAC stacking is a thin layer (one unit) of wurtzite (WZ) material. (b) HRTEM lattice image of a section of an InP nanowire. Gray stripes and black stripes are two different orientations of ZB segments. (c) and (d) are the close-up views of the lattice images marked in (b); they represent sections of the wires with low and high density of rotational twins, respectively. Short arrows in (c) and (d) indicate the locations of twin planes.

explained based on the mixture of extended ZB and WZ sections.[18] Theory also predicts that RT in a ZB crystal would change the electronic properties because a twin plane has WZ symmetry locally, thus creating a heterostructure[13,14] (Figure 1a). Despite the theoretical work, it is, however, a challenge to correlate the microscopic structure of RT to the electronic or optical properties induced by RT due to technical difficulties.

RT appears frequently in nanowires as a defect during the growth. TEM and HRTEM have been used to resolve individual lattices near the RT plane, and new growth techniques are being developed to control the growth dynamics of twinning planes.[4–6,9,15,19–21] A new type of superlattice based on RT heterojunction has been proposed and holds promise for many novel properties.[8] To reveal the effect of RT on the optical and electronic properties of the nanowire, we compared the PL spectrum from a single crystal ZB InP nanowire, and an InP nanowire with RT structure, and correlated the PL spectra to HRTEM images and diffraction patterns (DP) of the *same* nanowire. We found that RT is responsible for the observed blue shift of PL in randomly twinned InP nanowires.

Experimental Results. The InP nanowires were synthesized using metalorganic vapor phase epitaxy (MOVPE). Size-selected gold aerosol particles[22] with 40 nm diameter and a surface density of 1 μm^{-2} were used as growth catalysts on an InP (111)B surface. The nanowires were grown at 400 °C using trimethylindium (TMI) $(CH_3)_3In$, and phosphine, PH_3, as indium and phosphorus precursors, respectively. A phosphine molar fraction of 1.5×10^{-2} was used in a hydrogen carrier gas flow of 6 L/min at 100 mbar. At moderate TMI flows, the nanowires grow vertically (normally to the substrate) in the [111]B direction. However, with increased TMI flow the ⟨001⟩ and ⟨112⟩ growth directions also emerge. As discussed below, the ⟨001⟩ direction is of particular interest since it is inherently free from twinning defects and represents an ideal ZB single crystal.[4] The TMI molar fraction used for the reported nanowires was 2×10^{-5}, which is a factor of 4 higher than that used for producing vertical-only InP nanowires in the [111]B direction.

Scanning electron microscopy (SEM) images reveal that the InP nanowires are long (~8 μm) and uniform in diameter (80 nm) along the growth direction. The structure of InP nanowires was studied with TEM, using selected area electron diffraction (SAD) and HRTEM imaging. The SAD aperture used was 2 μm in diameter to correspond to the nominal size of the laser spot. As indicated in Figure 2, there is no change in the DP as this aperture is shifted along the wire. We focus here on the nanowires that grow in the ⟨111⟩ and ⟨001⟩ directions. The nanowire with ⟨001⟩ as growth direction were, as expected,[4] single crystal ZB, whereas the nanowires with ⟨111⟩ growth direction showed ZB structure with RT along the ⟨111⟩ growth direction. The HRTEM from a typical nanowire with RT is shown in Figure 1b−d. The thickness of ZB segments varies from a few monolayers to about 10 nm, in the same way as described for GaP nanowires by Johansson et al.[19]

Micro-PL measurements of individual InP nanowires were performed using a system consisting of a CCD-camera equipped spectrometer, an air-cooled continuous wave argon laser (488 nm), a long working distance objective, and a micro optical cryostat (Janis ST-500). In order to directly correlate the PL spectrum of a nanowire to its lattice structure, micro-PL and TEM have to be performed on the *same* single nanowire. Because of this, the substrate supporting the nanowires has to be TEM compatible. Initially,

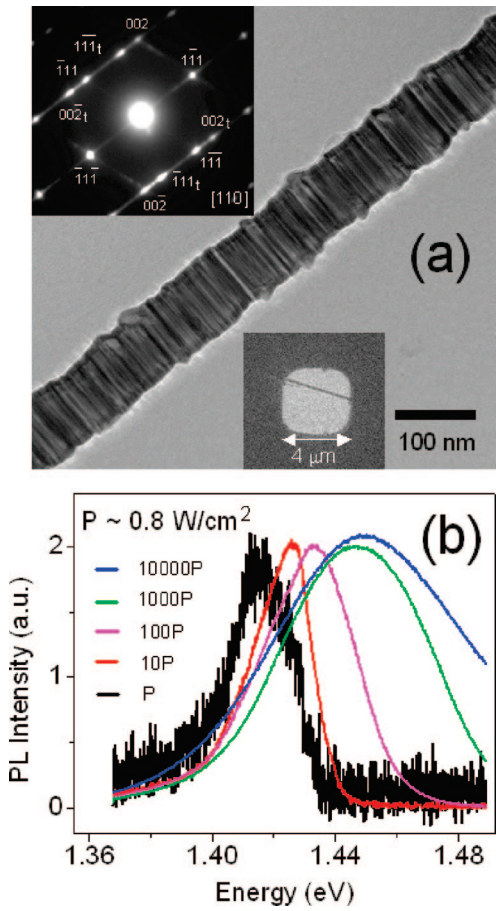

Figure 2. (a) TEM image of an InP nanowire with RT. Bottom inset: An InP nanowire on Si nitride membrane with both ends covered by Ti/Au film. Top inset: TEM diffraction pattern (DP) recorded along [110] zone axis. The DP reveals that it is a twinning ZB wire grown along the ⟨111⟩ direction. The twin DP can be viewed as a superposition of a ZB DP labeled without subscript t and a ZB DP with subscript t. DPs without t and with t share a rotation symmetry along the ⟨111⟩ direction, and they indicate ZB segments with two different orientations. (b) Photoluminescence (PL) of the nanowire in (a) under different excitation intensities at 7 K. The 488 nm laser was focused to a spot with ~2 μm diameter. The spectrum is normalized to the same scale for ease of comparison.

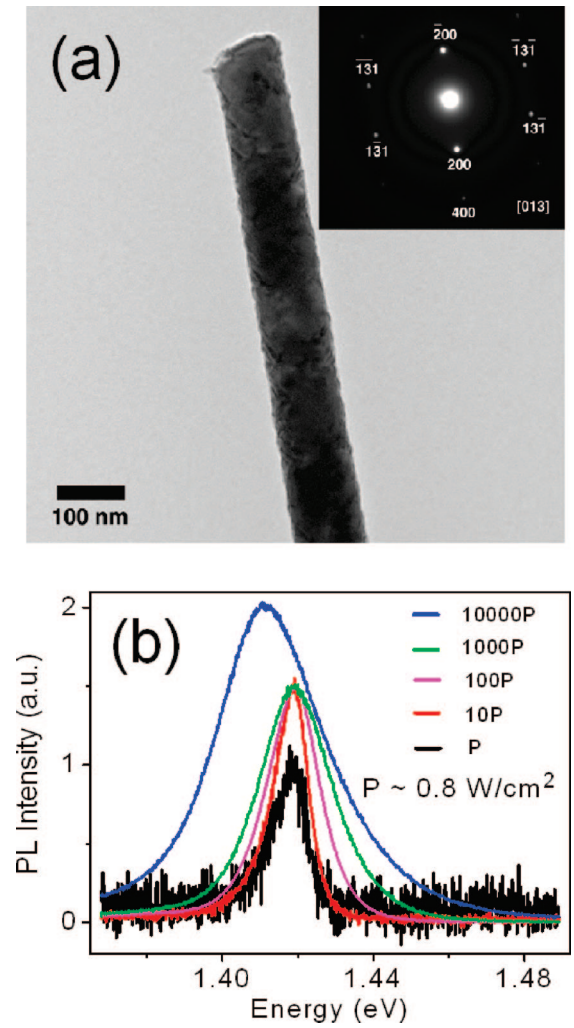

Figure 3. (a) TEM image of a single crystal ZB InP nanowire. Top right inset: TEM diffraction pattern recorded along the [013] zone axis, which reveals that the wire is single crystal (no twin planes) and the growth direction is ⟨001⟩. (b) Photoluminescence spectrum of the nanowire in (a) with different excitation intensities under the same conditions as in Figure 2b. The spectrum is scaled for ease of comparison.

a standard TEM perforated carbon grid was used to support the wires. Due to little thermal dissipation for the suspended wires in vacuum, wires as well as the carbon meshes were burned when the laser was focused on them. A suspended Si nitride membrane (50 nm thick, Ted Pella, Inc.) was found to provide better thermal dissipation for wires than a mesh grid. In order to further improve the thermal contact, we first placed the wires on the silicon nitride membrane and then evaporated a hole-patterned Ti/Au (5 nm Ti, 150 nm Au) film on the membrane. Nanowires to be measured were thus partly covered by a gold film at one or both ends (see the bottom inset of Figure 2a). This configuration is essential for taking a micro-PL spectrum at high excitation intensity without causing significant laser heating or burning of the nanowires. Because a focused electron beam may cause structural damage of the nanowires, micro-PL was performed before TEM imaging.

Using this technique, we studied two nanowires with different crystal structures, a single crystal ZB nanowire and a nanowire with a RT structure (throughout the nanowire). Figure 2 and Figure 3 show PL and TEM of these two nanowires. The electron diffraction of the nanowire in Figure 2a reveals that it has twinned ZB structure; similar DP was observed in many nanowires.[6,10,15] Due to the twinning structure, the TEM image in Figure 2a shows series of streaks, a manifestation of alternating orientations of ZB segments (Figure 1). The PL spectrum of this RT nanowire is strongly dependent on the excitation intensity. Its PL peak position starts at an energy slightly below the bandgap of bulk InP (1.42 eV at ~7 K, for ZB structure), then the peak position shifts to higher energy with increasing laser intensity. The nanowire in Figure 3 has a single crystal ZB structure, free of RT, as indicated by the indexed DP.[4,5] The single crystal nanowire shows a different PL characteristic than the nanowire with RT. The PL peak position at low excitation agrees well with the bandgap of bulk InP, and its peak

position does not shift with increasing excitation intensity. The increase of the line width is probably due to many body and hot carriers effects under strong optical excitation.[23] The red shift of PL at the highest intensity (~8000 W/cm^2) is believed to be due to laser heating of the nanowire. In addition, the single crystal ZB nanowire has a narrower spectral width than the nanowire with RT at the same excitation intensity. The above observations lead us to suggest that the RT structure in the InP nanowires is contributing to the blue shift of the PL peak position with increasing laser intensity.

In order to further reduce thermal effects on PL spectra, micro-PL was performed on nanowires dispersed on a silicon substrate, which has a high thermal conductivity. Similar to the nanowires observed with combined TEM and PL, we observed nanowires with hardly any spectral shift with increasing excitation power, as well as nanowires with large spectral shifts of several tens of millielectronvolts. As discussed above, these two behaviors were ascribed to single crystal ZB ⟨001⟩ nanowires and RT ⟨111⟩ nanowires, respectively. There were, however, also nanowires with a spectral behavior that could not be described as either of these two types. These nanowires had for instance spectral shifts that were clearly smaller than the tens of millielectronvolts observed for nanowires with RT structure or different spectral behavior at different positions of the nanowire. These nanowires might not have a RT structure throughout the entire length of the nanowire, but the reason for the different behaviors is not completely clear.

Figure 4a shows the peak energy as a function of excitation power for a nanowire exhibiting a large power dependent spectral blue-shift. This type of nanowire is assumed to be of the same type as the RT ⟨111⟩ nanowire shown in Figure 2. The peak energy increased nearly linearly with the logarithm of the excitation power. Figure 4b shows the corresponding total integrated PL intensity of the nanowire in Figure 4a. The PL intensity, I, showed no sign of saturation and could be fitted with $I = CP^{\alpha}$, where C is a constant, P is the excitation power, and $\alpha = 0.91$. This nearly linear behavior indicates that the optical transition responsible for the PL is not impurity related.

Interpretation and Discussion. A similar excitation power dependent blue-shift of PL was previously reported in quantum wells with staggered band alignment and was observed by many authors.[24–28] We believe that the spectral blue-shift observed in our RT nanowires is a manifestation of the latter type of band alignment of the heterostructures formed by the alternating WZ and ZB sections. The quantum confinement effect can be neglected due to the large nanowire diameter (~80 nm). The band gaps of ZB and WZ InP, as well as the heterojunction band offsets, have been calculated in ref 7. The larger band gap of WZ InP has been verified in recently synthesized WZ InP nanowires.[29–31] The calculations in ref 7 predict that the band gap of WZ InP is higher than that of ZB InP by 84 meV and that a WZ/ZB InP heterojunction has staggered band alignment with the WZ conduction band 129 meV above the ZB conduction band, and the WZ valence band 45 meV above that of ZB (Figure 5a). As discussed above (Figure 1), a twin plane introduces one unit of WZ structure in the surrounding ZB lattice.[8,10,13–15] Therefore twinned nanowires can be regarded as a series of ZB wells with varying widths separated by thin WZ barriers.

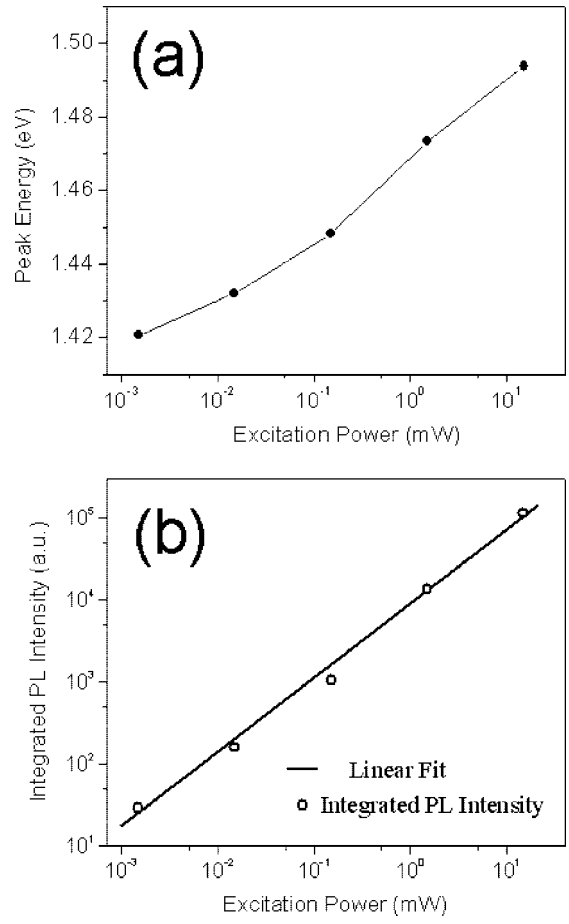

Figure 4. (a) Peak energy of the photoluminescence and (b) total integrated intensity of photoluminescence vs excitation power for a twinning nanowire on a silicon substrate at 7 K. The line in (a) is a guide to the eyes. A 488 nm laser was focused to a spot of ~2 μm in diameter.

The PL blue shift in quantum well heterostructures with staggered band alignment was explained as follows.[24–28] Photoexcited electrons and holes are spatially separated across the heterojunction. This space charge induces an electric field and band bending, which modifies the electron and hole energy levels via the Stark effect, thus leading to the PL blue shift. Furthermore, because of the spatial separation of electrons and holes, their recombination time will increase. However it could not be measured in our twinned InP nanowires using time-resolved PL due to the low signal level from a single nanowire. At high excitation power, photoexcited electrons and holes begin to occupy the higher energy subbands, and a band-filling effect takes place.[23] Thus both band bending and band filling are expected to contribute to the PL blue-shift. In analogy to the interpretation of the PL blue-shift in staggered quantum well heterostructures, we propose that band-bending is responsible for the weak blue-shift at relatively low excitation power, whereas the band filling effect is responsible for the stronger blue-shift at higher excitation power. The existence of two

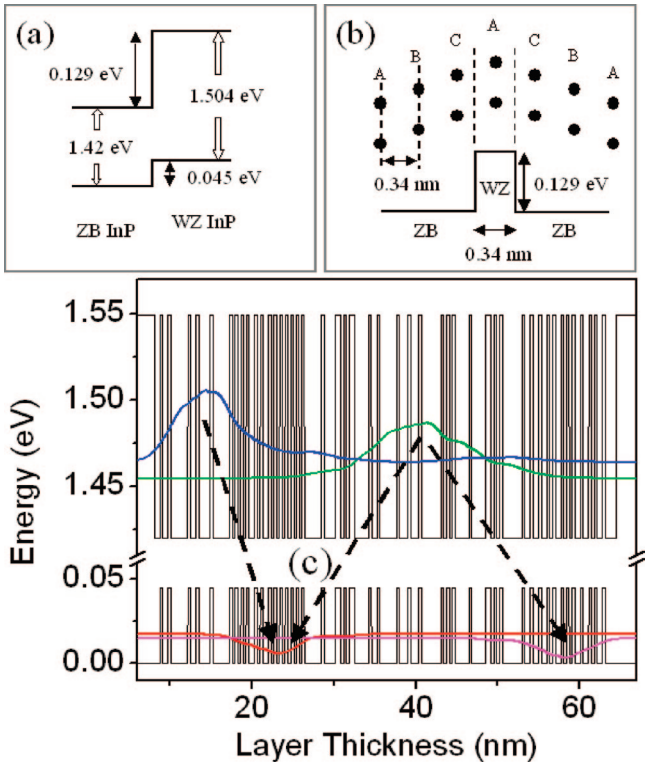

Figure 5. (a) Band alignment between ZB InP and WZ InP according to ref 7. (b) Conduction band potential profile and the corresponding thickness of WZ and ZB layers near a twin plane used in the calculation. The CAC stacking is one unit of WZ InP; however, because the left layer C also belongs to the left BCA stacking (ZB), the right layer C belongs to the right ACB layer (ZB), so the effective thickness of WZ section is half of the thickness of CAC layer, which is ~0.34 nm. (c) Potential profile, moduli squared of the wave functions of electrons and holes, and their energy levels for the RT wire shown in Figure 1b. The sequence of WZ/ZB layers and their thickness are defined in (b) and according to lattice image in Figure 1b. The dashed arrows indicate electron–hole recombination.

different effects results in a kink in the curve of peak energy shift versus excitation power.[24–27] In our twinned InP nanowires, as indicated by TEM in Figure 1b, twinning occurs nonperiodically along the nanowire. In some regions, there is a long segment of ZB-InP-rich structure, due to the large spacing between twin planes (see Figure 1c), while in other regions, there is a WZ-InP-rich segment because of closely spaced twin planes (Figure 1d). As a result, we can treat the RT nanowire as a de facto random nanowire superlattice of ZB and WZ segments.

In Figure 5c the potential profile according to the stacking sequence from the TEM image in Figure 2b is plotted together with the electron and hole probability densities. In the calculation, the wave functions of electron and hole are described by the envelope function approximation and solved using the shooting method.[32,33] The in-plane momentum perpendicular to ⟨111⟩ is neglected, and the effective masses of electrons ($0.073m$, m is the electron mass in vacuum) and heavy holes ($0.58m$) in ZB InP are used.[34] The electron effective mass in WZ InP has not been reported in the literature; we have scaled it in accordance with the bandgap change from ZB InP to WZ InP using Kane's theory. The heavy hole mass change is expected to be small and inconsequential in affecting the wavefunction localization shown in Figure 5. As can be seen, electrons in the ground state and low excited states are confined in regions with a large fraction of ZB InP, while the holes are confined in WZ-InP-rich regions, thus strongly favoring PL transitions that are diagonal in real space, leading to a blue shift with increased photoexcitation. However, due to the variation of twinning spacing, we have a distribution of ZB-rich and WZ-rich regions with various thicknesses, which may contribute to a broader PL line width and a lack of a clear kink in Figure 4a.[24–27] The observation that the peak energy of the PL spectrum at low excitation power is close to the bandgap of ZB InP (Figure 2b) also agrees with the calculations shown in Figure 5c.

In conclusion, we have experimentally observed the effect of rotation twinning on the optical properties of ZB InP nanowires. In order to establish the correlation between the observed optical properties with the twinning structure, we developed a new type of substrate that has made it possible to perform micro-PL with high excitation power and HRTEM on the same single nanowire. Using this technique, we have observed a different PL behavior for RT InP nanowires compared with single crystal ZB InP nanowires. Our observations were qualitatively explained based on the staggered band alignment between ZB- and WZ-InP. Because the results of higher bandgap of the WZ structure, and the staggered band alignment between ZB/WZ, apply to nearly all direct bandgap semiconductors,[7,28] similar blue-shift of PL is expected in other RT semiconductor nanowires such as InAs, ZnS, or ZnSe. Our findings support early theoretical studies that rotation twinning introduces a heterojunction in a chemically homogeneous material,[13,14] thus creating new opportunities for materials engineering employing controlled twin formation.[8]

Acknowledgment. The authors thank Dr. Qijie Wang for assistance in the wavefunction calculations and Professor Mats-Erik Pistol, Mariano Zimmler, Dr. Mikhail Belkin, Dr. Laurent Diehl, and Dr. Christian Pflügl for many valuable discussions. Partial financial support from the National Science Foundation Nanoscale Science and Engineering Center at Harvard is gratefully acknowledged. The support of the Center for Nanoscale Systems (CNS) at Harvard University is also gratefully acknowledged. Harvard CNS is a member of the National Nanotechnology Infrastructure Network (NNIN). This research was performed within the Nanometer Structure Consortium at Lund University with financial support from the Swedish Research Council (VR), the Swedish Foundation for Strategic Research (SSF), the Knut and Alice Wallenberg Foundation (KAW), and from the European Union via the project NODE 015783.

References

(1) (a) Huang, Y.; Lieber, C. M. *Pure Appl. Chem.* **2004**, *76*, 2051. (b) Lieber, C. M. *MRS Bull.* **2003**, *28*, 486.

(2) Samuelson, L.; Thelander, C.; Björk, M. T.; Borgström, M.; Deppert, K.; Dick, K. A.; Hansen, A. E.; Mårtensson, T.; Panev, N.; Persson, A. I.; Seifert, W.; Sköld, N.; Larsson, M. W.; Wallenberg, L. R. *Physica E* **2004**, *25*, 313.

(3) Pryor, C. E.; Pistol, M. E. *Phys. Rev. B* **2005**, *72*, 205311.
(4) (a) Krishnamachari, U.; Borgstrom, M.; Ohlsson, B. J.; Panev, N.; Samuelson, L.; Seifert, W.; Larsson, M. W.; Wallenberg, L. R. *Appl. Phys. Lett.* **2004**, *85*, 2077. (b) Björk, M. T.; Ohlsson, B. J.; Sass, T.; Persson, A. I.; Thelander, C.; Magnusson, M. H.; Deppert, K.; Wallenberg, L. R.; Samuelson, L. *Appl. Phys. Lett.* **2002**, *80*, 1058–1060.
(5) Xiong, Q. H.; Wang, J.; Eklund, P. C. *Nano Lett.* **2006**, *6*, 2736–2742.
(6) Bhunia, S.; Kawamura, T.; Fujikawa, S. *Thin Solid Films* **2004**, *464*, 244–247.
(7) Murayama, M.; Nakayama, T. *Phys. Rev. B* **1994**, *49*, 4710–4724.
(8) (a) Ikonic, Z.; Srivastava, G. P.; Inkson, J. C. *Phys. Rev. B* **1995**, *52*, 1474–1476. (b) Bandić, Z. Z.; Ikonić, Z. *Phys. Rev. B* **1995**, *51*, 9806–9812. (c) Ikonic, Z.; Srivastava, G. P.; Inkson, J. C. *Surf. Sci.* **1994**, *307–309*, 880–884.
(9) Hibino, H.; Ogino, T. *Mater. Sci. Eng., B* **2001**, *87*, 214–221.
(10) Williams, D. B.; Carter, C. B. *Transmission electron microscopy: a textbook for materials science*; Plenum Press: New York, 1996.
(11) Trigunayat, G. C. *Solid State Ionics* **1991**, *48*, 3–70.
(12) Yeh, C. Y.; Lu, Z. W.; Froyen, S.; Zunger, A. *Phys. Rev. B* **1992**, *46*, 10086–10097.
(13) Birman, J. L. *Phys. Rev.* **1959**, *115*, 1493–1505.
(14) Northrup, J. E.; Cohen, M. L. *Phys. Rev. B* **1981**, *23*, 2563–2566.
(15) Hiruma, K.; Yazawa, M.; Katsuyama, T. *J. Appl. Phys.* **1995**, *77*, 447–462.
(16) Ellis, S. G. *Phys. Rev.* **1958**, *109*, 1860.
(17) Lempicki, A. *Phys. Rev.* **1959**, *113*, 1204.
(18) Neumark, G. F. *Phys. Rev.* **1962**, *125*, 838.
(19) Johansson, J.; Karlsson, L. S.; Svensson, C. P. T.; Martensson, T.; Wacaser, B. A.; Deppert, K.; Samuelson, L.; Seifert, W. *Nat. Mater.* **2006**, *5*, 574–580.
(20) Hao, Y.; Meng, G.; Wang, Z. L.; Ye, C.; Zhang, L. *Nano Lett.* **2006**, *6*, 1650–1655.
(21) Wu, R. B.; Pan, Y.; Yang, G. Y. *J. Phys. Chem. C* **2007**, *111*, 6233–6237.
(22) Magnusson, M. H.; Deppert, K.; Malm, J. O.; Bovin, J. O.; Samuelson, L. g. *J. Nanopart. Res.* **1999**, *1*, 243–251.
(23) Cingolani, R.; Ploog, K. *Adv. Phys.* **1991**, *40*, 535–623.
(24) Fouquet, J. E.; Minsky, M. S.; Rosner, S. J. *Appl. Phys. Lett.* **1993**, *63*, 3212–3214.
(25) Liu, Q.; Derksen, S.; Lindner, A.; Scheffer, F.; Prost, W.; Tegude, F.-J. *J. Appl. Phys.* **1995**, *77*, 1154–1158.
(26) Benyattou, T.; Garcia, M. A.; Moneger, S. *Appl. Surf. Sci.* **1993**, *63*, 197–201.
(27) Luo, X. D.; Hu, C. Y.; Xu, Z. Y.; Luo, H. L.; Wang, Y. Q.; Wang, J. N.; Ge, W. K. *Appl. Phys. Lett.* **2002**, *81*, 3795–3797.
(28) Lu, X. H.; Yu, P. Y.; Zheng, L. X. *Appl. Phys. Lett.* **2003**, *82*, 1033–1035.
(29) Mohan, P.; Motohisa, J.; Fukui, T. *Nanotechnology* **2005**, *16*, 2903–2907.
(30) Mattila, M.; Hakkarainen, T.; Mulot, M. *Nanotechnology* **2006**, *17*, 1580–1583.
(31) Tragardh, J.; Persson, A. I.; Wagner, J. B.; Hessman, D.; Samuelson, L. *J. Appl. Phys.* **2007**, *101*, 123701.
(32) Bastard, G. *Wave mechanics applied to semiconductor heterostructures*; Les éditions de physique; Les Ulis: France, 1988.
(33) Stoer, J.; Bulirsch, R. *Introduction to Numerical Analysis*; Springer-Verlag: New York, 1980 . (see Section 7.3).
(34) Yu, P. Y.; Cardona, M. *Fundamentals of Semiconductors*; Springer: New York, 2001.

NL072921E